Bull. Chem. Soc. Ethiop. **2025**, 39(2), 341-350.
DOI: https://dx.doi.org/10.4314/bcse.v39i2.12

ISSN 1011-3924
Printed in Ethiopia
Online ISSN 1726-801X

EXPLORING THE HALF-METALLIC BEHAVIOR AND SPINTRONIC POTENTIAL OF Cr-DOPED CaTe

M. Drissi El Bouzaidi[1,2,3*] and R. Ahl Laamara[1,2]

[1]LPHE-Modeling and Simulations, Faculty of Sciences, Mohammed V University in Rabat, Morocco
[2]Centre of Physics and Mathematics, CPM- Morocco, Mohammed V University in Rabat, Morocco
[3]National School of Architecture of Tétouan (ENA), Tétouan, Morocco

(Received August 21, 2024; Revised October 1, 2024; Accepted October 25, 2024)

ABSTRACT. The pursuit of miniaturized, high-performance electronic devices has intensified research into novel materials with extraordinary properties. While semiconductors lead the way in optoelectronics and energy harvesting, the burgeoning field of spintronics utilizing electron charge and spin promises revolutionary advances in information processing and storage. A critical component of spintronics is identifying materials with half-metallic behavior, characterized by complete spin polarization at the Fermi level. This study explores chromium (Cr)-doped CaTe as a candidate for half-metallic behavior. Using advanced computational techniques, we investigate the impact of Cr doping on the electronic and magnetic properties of CaTe. Our findings reveal that Cr-doped CaTe exhibits significant crystal field splitting and exchange splitting energies, leading to robust magnetic properties and half-metallic behavior across varying doping concentrations. Notably, the Curie temperature of Cr-doped CaTe exceeds room temperature starting from a 14% Cr concentration, highlighting its practical viability for spintronic applications. The results underscore the potential of Cr-doped CaTe for integration into spintronic devices, offering insights into the electronic structure and magnetic interactions essential for developing next-generation spintronic technologies.

KEY WORDS: Half-metallic behavior, Spintronics, Chromium doping, Curie temperature, Magnetic properties, CaTe (Calcium telluride).

INTRODUCTION

The drive for miniaturized, high-performance electronic devices has spurred extensive research into novel materials with exceptional properties. Semiconductors, notable for their tunable electronic characteristics, are at the forefront of technological progress, with applications spanning optoelectronics, electronics, and energy harvesting systems [1]. Nevertheless, the relentless demand for faster, more efficient, and denser information processing and storage solutions has pushed the exploration of new paradigms. Spintronics, utilizing both the charge and spin of electrons, presents a promising path to overcome the limitations of traditional electronics [2].

A key aspect of spintronic device development is the identification and use of materials exhibiting half-metallic behavior. Such materials have a unique electronic structure characterized by complete spin polarization at the Fermi level: one spin channel shows metallic conductivity, while the other behaves as an insulator or semiconductor [3]. This distinct property holds the potential for significantly enhanced device performance, lower power consumption, and increased data storage density compared to conventional electronics. Despite significant theoretical and experimental progress, achieving practical half-metallic materials at room temperature remains challenging.

*Corresponding authors. E-mail: m.elbouzaidi@enatetouan.ac.ma

Calcium chalcogenides CaX compounds (where X = S, Se, and Te), classified as group II VI alkali-earth calcium chalcogenides, exhibit a rock-salt (B1) structure under ambient conditions [4, 5]. Under high pressure, they transition to the CsCl-type structure (B2) and become metallic [6]. Recent studies have extensively examined these materials. Experimentally, Luo *et al.* [6] employed energy-dispersive X-ray diffraction techniques to investigate their behavior under high pressure, revealing that CaS and CaSe transition from the NaCl phase to the CsCl phase at pressures of 40 and 38 GPa, respectively. Notably, CaTe exhibits a more complex phase transformation: it first shifts from the NaCl phase to an intermediate state involving a mixture of NaCl and MnP phases at 25 GPa, and subsequently transitions to the CsCl phase above 33 GPa. This intricate behavior underscores the unique properties of CaTe compared to the other chalcogenides.

Supporting these findings, Rakesh Roshan *et al.* [7] used a plane wave pseudopotential approach to theoretically con rm that CaS and CaSe undergo a first-order structural phase transition from the rock-salt (B1) to the CsCl-type (B2) structure at 34.9 GPa and 31.8 GPa, respectively, aligning with the experimental data [6]. Additionally, the elastic constants of CaS and CaSe in the rock-salt (B1) structure have been determined, showing mechanical stability at ambient conditions [8]. Further studies employed pseudopotential and tight-binding methods to assess the properties of CaX (X = S, Se, and Te) [9, 10]. The linear optical properties of these compounds were investigated using the FP-LAPW method [11], while their high-pressure structural, elastic, and electronic properties were computed in [12]. These studies reveal that the compounds exhibit semiconducting behavior with a wide indirect band gap (Γ-X), making them promising for optoelectronic applications, including thermoluminescence, photoluminescence, and phosphorescence.

However, the intrinsic properties of CaX do not naturally support the spin-based functionalities needed for spintronic devices. To harness the potential of CaTe for spintronics, the concept of diluted magnetic semiconductors (DMS) is promising. Introducing magnetic impurities, such as transition metals, into the semiconductor host can induce magnetic properties and potentially modify the electronic structure to achieve the desired spin-dependent functionalities [13, 14].

Numerical simulations are crucial for deepening our understanding of CaTe and similar materials, offering a cost-effective way to adjust parameters and address specific requirements. Methods like DFT, DFT+U, and DFPT have become indispensable in materials science, enabling researchers to predict the properties of compounds before conducting experiments, particularly for those with distinct features. In many instances, integrating theoretical models with experimental findings is key to unravelling complex phenomena, which ultimately aids in designing materials with customized properties for advanced technological uses [15-17].

This study explores the potential of chromium (Cr)-doped CaTe as a promising candidate for halfmetallic behavior. Using advanced computational techniques, we aim to elucidate the impact of Cr doping on the electronic and magnetic properties of CaTe. Our investigation focuses on identifying conditions under which half-metallic behavior can be realized and evaluating the potential of Cr-doped CaTe for integration into spintronic devices. A comprehensive understanding of the mechanisms governing the electronic structure and magnetic properties of this system is essential for developing novel spintronic devices with superior performance and efficiency. The manuscript is organized as follows: The next section details the calculation methods and the structural properties of CaTe. Section 3 discusses the results obtained, including electronic properties, band structure and density of states, formation energy, stable phase, magnetic moment, and Curie temperature for various concentrations of transition metals, for pure as well as Cr doped CaTe.

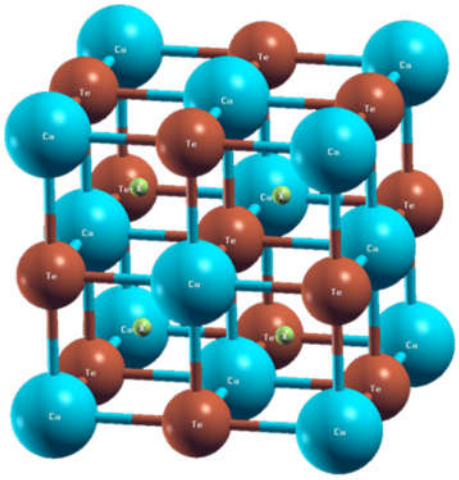

Figure 1. Unit cell of CaTe.

Methodology and structural analysis

Due to its high capacity, speed, and accuracy in handling disorder in materials [18, 19], the self-consistent KKR Green's function method [20-23] is employed to calculate the structural, electronic, and magnetic properties of the host semiconductor CaTe.

CaTe features a halite (rock salt) structure and crystallizes in the cubic $Fm^{-}3m$ (225) space group, as illustrated in Figure 1. In this structure, Ca^{2+} ions are coordinated with six equivalent Te^{2-} ions, forming edge- and corner-sharing $CaTe_6$ octahedral with bond lengths of 3.33 Å. Similarly, Te^{2-} ions bond with six Ca^{2+} ions. The bonding in CaTe exhibits an ionic character with notable covalent aspects due to the significant electronegativity difference between Ca and Te, which exceeds 0.5 on the Pauling scale. The crystal structure of CaTe is characterized by Wyckoff positions where Ca is located at (0, 0, 0) and Te at (0, 1/2, 0).

The disordered system is effectively described using the CPA method, which evaluates the average electronic properties rather than those of individual doping elements [24]. For these calculations, the generalized gradient approximation (GGA) based on Perdew, Burke, and Ernzerhof (PBE) parameterization [25] is used for the exchange-correlation energy functional. The potentials are treated as muffin-tin (MT), where they are spherically symmetric inside the atomic sphere and constant in the interstitial regions. Electronic wave functions are computed with angular momentum quantum numbers defined up to $\ell = 2$ for d electrons. The first Brillouin zone is sampled with 500 K-points, and relativistic effects are considered using the scalar relativistic approximation (SRA) for the valence states. The PBE-KKR-CPA is implemented in the MACHIKANEYAMA2002 package produced by Akai of Osaka University, Japan [18].

RESULTS AND DISCUSSION

We begin our investigation by analyzing the structural properties of CaTe. This material adopts a halite (rock-salt) structure, where calcium (Ca) and tellurium (Te) atoms are arranged in a cubic $Fm^{-}3m$ space group. The energy optimization method identifies the lattice parameter that minimizes the total energy, which is determined to be $a_0 = 6.663$ Å as shown in Figure 2. This value shows excellent agreement with the theoretical results found in [28].

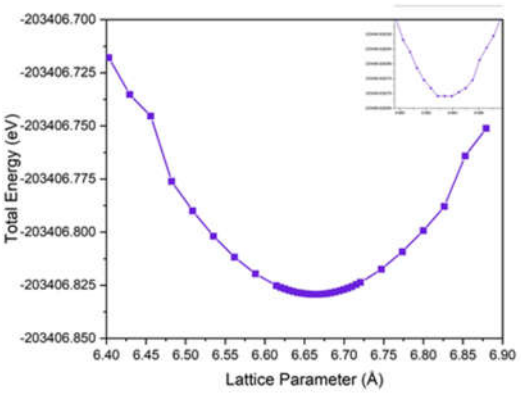

Figure 2. Optimization of the parameter lattice of CaTe.

The electronic properties are further explored through the calculation of the total density of states (TDOS) and partial density of states (PDOS) for CaTe in Figure 3(a). TDOS is presented per unit cell, while PDOS is computed per atomic orbitals. Near the Fermi level, a substantial band gap of Eg = 1.59 eV is observed, despite our detailed analysis, we do not find clear band gap values for CaTe in literature. This highlights the need for further experimental and theoretical studies to accurately determine the band gap. Observations indicate that the Fermi level intersects the valence band, which classifies CaTe as a p-type semiconductor. This positioning of the Fermi level suggests that holes dominate the charge carriers in this material.

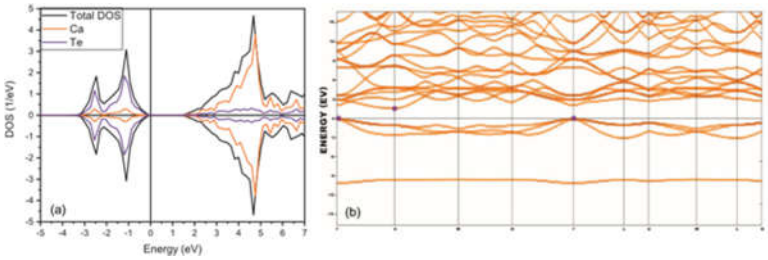

Figure 3. (a) TDOS and PDOS of CaTe and (b) band structure of CaTe.

The indirect band gap in CaTe is positioned at Γ in the valence band and at the X point in the conduction band Figure 3(b). This suggests limited efficacy of CaTe as a light emitter due to the necessity of phonons for inter-band transitions, resulting in a low transition rate. However, CaTe can function effectively as a light absorber. For instance, when CaTe absorbs photons with energy exceeding Eg, electrons can transition from the valence band at Γ to the conduction band at the X point. The corresponding photon wavelength λ, calculated from Eg, is 780 nm, placing it within the visible spectrum. This implies that CaTe can absorb visible and infrared light, making it a potential material for optoelectronic applications.

The non-magnetic nature of pure CaTe is evident from the symmetry between the spin-up and spin-down DOS (Figure 3(a)). This symmetry indicates that there is no net magnetic moment in the material, as the contributions from spin-up and spin-down electrons cancel each other out. However, when CaTe is doped with transition metals, particularly chromium (Cr), the situation

changes significantly. Doping introduces localized magnetic moments due to the unpaired d-electrons of the transition metal atoms.

We varied Cr concentrations from 2% to 25%, systematically investigating the resulting changes in electronic and magnetic behavior of the system. As Cr atoms replace Ca atoms in the lattice, their d-electrons interact with the electronic states of CaTe, leading to the emergence of magnetic properties. The DOS analysis reveals that the introduction of Cr results in a distinct asymmetry between the spin-up and spin-down channels near the Fermi level (Figure 4).

At lower doping concentrations (around 2%), the Cr impurities induce a small magnetic moment in the system. This is evident from the slight splitting of the DOS in the spin-up and spin-down channels. As the concentration of Cr increases, the magnetic interaction between Cr atoms becomes stronger, leading to a more pronounced splitting in the DOS. This indicates an increase in the net magnetic moment of the system.

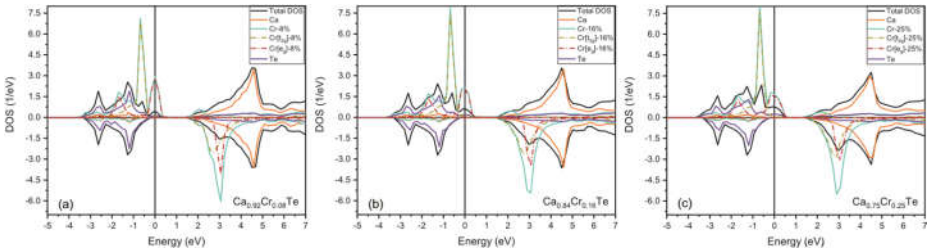

Figure 4. Total and partial density of states (DOS) of Ca1-xCrxTe.

By the time we reach a Cr concentration of 25%, the DOS shows a significant asymmetry between the spin-up and spin-down states, indicating a robust magnetic order. The TDOS and PDOS for the 3d orbitals of Cr-doped CaTe reveal that the magnetic properties are primarily due to the Cr-3d states, which dominate near the Fermi level. The increasing concentration of Cr not only enhances the magnetic moment but also modifies the electronic structure, leading to the observed transformation in the electronic and magnetic behavior of the system.

As we can see from Figure 4, the TDOS and PDOS for the 3d orbitals of Cr-doped CaTe reveal a significant change. Notably, at the Fermi level, only one spin direction appears in the semiconducting gap, indicating half-metallic behavior. This half-metallicity is consistent across all doping concentrations, from 2% to 25%.

The sharp peaks of the 3d electronic states crossing the Fermi level result in a net magnetization. These peaks indicate the localized character of the d-electron DOS, contrasting with the wider and atter p-electron DOS. The localized impurity states, combined with the delocalized states in the conduction and valence bands, contribute to the magnetic properties of the doped system.

Substituting Ca sites with Cr impurities leads to a splitting of the d-orbitals into t2g and eg sub-orbitals due to the octahedral crystal field effect. The crystal field splitting energy ΔCR and exchange splitting energy ΔEX are calculated, showing significant splitting caused by the introduction of Cr impurities. Cr, with its 5 d-orbitals electrons, loses one electron to become Cr^{+}, filling the up-spin direction of the t_{2g}-orbital and partially filling the eg-orbital (Figure 5).

The partially filled eg-orbital, positioned at the Fermi level is the origin of the half-metallicity in the system. This positioning results in one spin direction being present at the Fermi level, leading to metallic behavior for one spin channel while maintaining semiconducting behavior for the other. The down-spin t_{2g} and e_g sub-orbitals remain empty and are therefore located in the conduction band, further contributing to the overall magnetic properties of the doped system.

In Table 1, we display the magnitude of the crystal field splitting, which is calculated using the equation $\Delta_{CR} = E(t_{2g}^{\wedge+}) - E(e_g^{\wedge+})$. This calculation provides an insight into the extent of the splitting of the d-orbitals caused by the crystal field effect in the octahedral arrangement. Furthermore, we evaluate the exchange splitting energy, which quantifies the separation between the spin-up and spin-down states of the t-orbitals. This is determined using the relation $\Delta_{EX} = E(t_{2g}^{\wedge+}) - E(t_{2g}^{\wedge-})$. The exchange splitting energy is crucial for understanding the magnetic behavior of Cr-doped CaTe, as it directly influences the degree of spin polarization and the resultant magnetic properties. By analyzing these energies, we can better comprehend the electronic structure and magnetic interactions within the doped material, which are essential for predicting its potential performance in spintronic applications. The data presented in Table 1, thus provides a comprehensive overview of the effects of Cr doping on the electronic and magnetic characteristics of CaTe, highlighting the significance of both crystal field and exchange splitting energies in this context.

Table 1. Crystal field and exchange splitting for $Ca_{1-x}Cr_xTe$.

Cr(%)	Δ_{CR} (eV)	Δ_{EX} (eV)
8%	0.698	3.363
16%	0.684	3.431
25%	0.488	3.551

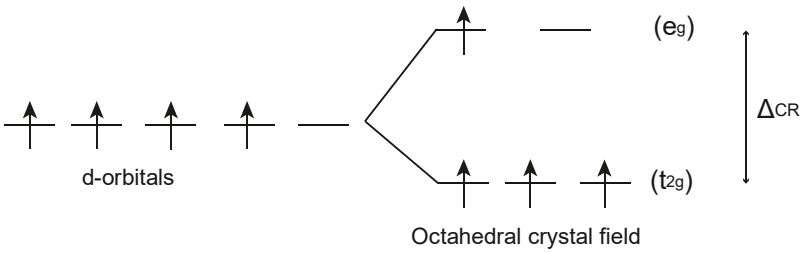

Figure 5. Electron configuration of Cr^+ impurities in CdTe.

The double exchange mechanism is a crucial concept in understanding ferromagnetism in transition metal oxides and related materials. It arises from the interaction between localized magnetic moments of transition metal ions and delocalized electrons, which can hop between these ions. In this mechanism, the presence of a mobile electron allows for a cooperative alignment of the spins of neighboring ions, effectively facilitating the exchange interaction. For instance, in systems like Cr-doped CaTe, the d-electrons of the Cr ions interact with the p-states of the surrounding anions, leading to a stabilization of ferromagnetic order. This phenomenon is characterized by the alignment of spins resulting from the virtual hopping of electrons between sites with different spin orientations. Analyzing the PDOS of the d-orbitals of Cr as a function of concentration, we observe in Figure 6, a double exchange mechanism due to hybridization between Te(2p) and Cr(3d) orbitals. This interaction is short-range and becomes significant as impurity concentrations increase. The doping process does not alter the covalent nature of the bonding, as the difference in electronegativity remains above 0.5, ensuring the system's overall stability. As a result, the double exchange mechanism plays a significant role in enhancing magnetic ordering and is essential for the development of materials with desirable spintronic properties, such as high Curie temperatures and robust magnetism.

The magnetic contribution from Cr impurities is significant, with impurity moment values around 4.2 μB/atom as shown in Table 2. This large magnetic moment per Cr atom is indicative

of the strong localized magnetic moments introduced by the Cr dopants. These moments arise from the unpaired d-electrons of Cr, which, when substituted into the CaTe lattice, interact strongly with the surrounding Te atoms, leading to the observed magnetic behavior.

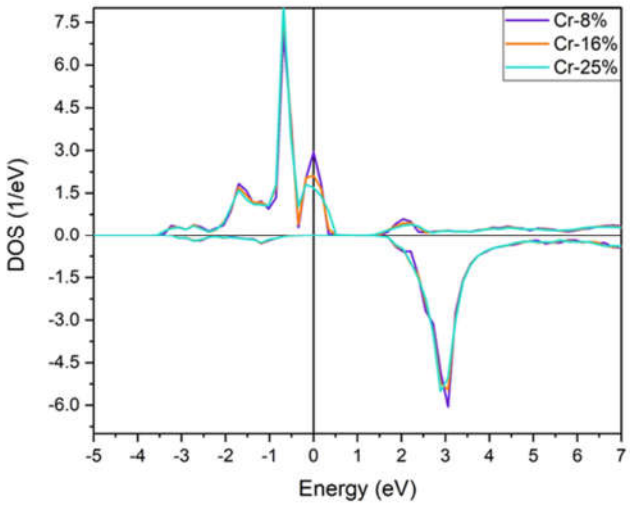

Figure 6. PDOS comparison of d-orbitals of Cr in $Ca_{1-x}Cr_xTe$ in terms of concentrations.

As we increase the concentration of Cr in CaTe, the total magnetization of the system shows a linear increase. This linear relationship between Cr concentration and total magnetization underscores the dominant role of Cr in inducing and enhancing magnetism within the host material. It suggests that each additional Cr atom consistently contributes its magnetic moment to the overall magnetization, without significant interactions that might otherwise reduce the effectiveness of individual magnetic moments, as we can see in Table 2.

This linear trend is evident in our calculated total magnetization values, as shown in Figure 7. At lower concentrations, the Cr atoms are relatively isolated from each other, and their magnetic moments add up independently. As the concentration increases, the interaction between Cr atoms may start to become more significant, but the linear increase in total magnetization indicates that these interactions do not lead to any significant frustration or reduction in the net magnetic moment.

Table 2. Local moments for $Ca_{1-x}Cr_xTe$ as a function of concentrations.

Cr(%)	Cr moment (μB/atom)	Ca moment (μB/atom)	Te moment (μB/atom)
8%	4.235	-0.00054	-0.02988
16%	4.242	-0.00059	-0.06062
25%	4.246	-0.00036	-0.09661

The robustness of the induced magnetization across varying Cr concentrations highlights the potential of Cr-doped CaTe for applications in spintronics. The ability to tune the magnetic properties of the material by adjusting the Cr concentration provides a valuable tool for designing devices with specific magnetic characteristics. This tunability, combined with the high magnetic

moment per Cr atom, makes Cr-doped CaTe a promising material for future technological applications where magnetic properties are crucial.

To study the stabilization of magnetic states, we calculate the total energy difference ΔE between the spin glass phase and ferromagnetic states. For concentrations above 5%, ΔE, indicating that the ferromagnetic phase is the stable phase starting from this value. This energy difference suggests that beyond 5% Cr concentration, the system energetically favors a ferromagnetic alignment over a disordered spin glass state.

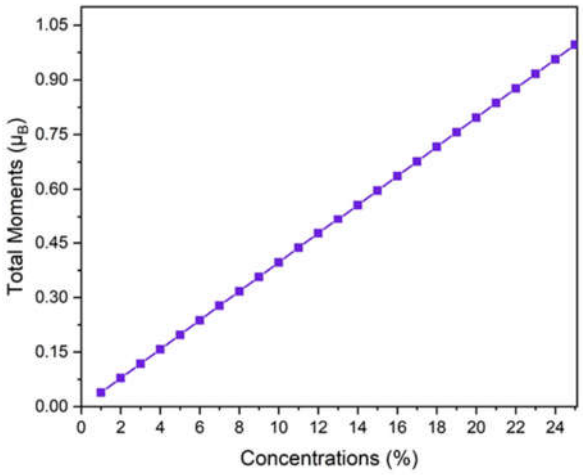

Figure 7. Total moments for $Ca_{1-x}Cr_xTe$.

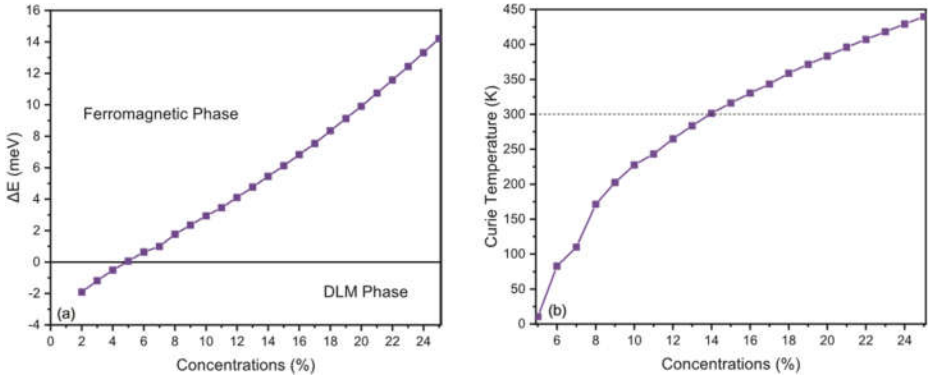

Figure 8. Curie temperature TC (in K) against Cr doping concentrations in $Ca_{1-x}Cr_xTe$.

Consequently, the Curie temperature T_c is determined for various Cr concentrations. The Curie temperature represents the temperature above which the material loses its permanent magnetic properties and becomes paramagnetic. At 5% Cr concentration, T_c is calculated to be 10.56 K, which is relatively low. However, as the Cr concentration increases, T_c also increases

significantly, reaching a maximum of 439.93 K at 25% Cr concentration. This maximum T_c indicates a strong ferromagnetic interaction within the material at higher Cr doping levels.

Interestingly, the T_c values exceed room temperature starting from 14% Cr concentration, which is approximately 298 K. This characteristic is particularly important for practical applications, as it means the material can maintain its ferromagnetic properties at ambient conditions without requiring additional cooling or heating mechanisms.

The ability to maintain ferromagnetic properties above room temperature is crucial for practical and commercial applications in the field of spintronics. Devices based on spintronic principles rely on the manipulation of electron spins, which in turn depend on the magnetic properties of the materials used. The high T_c values of Cr-doped CaTe ensure consistent performance in such devices, making it a promising candidate for spintronic applications at ambient conditions. This stability facilitates the design of more efficient and reliable spintronic devices, enhancing their potential for widespread adoption in technologies such as magnetic sensors, memory devices, and quantum computing components.

CONCLUSION

This study has thoroughly examined the potential of Cr-doped CaTe as a candidate for half-metallic behavior, essential for spintronic applications. Our computational analysis reveals that doping CaTe with chromium induces significant crystal field and exchange splitting energies, leading to robust magnetic properties and half-metallicity. We observed that Cr doping transforms the non-magnetic CaTe into a material with pronounced magnetic order, with the total magnetization increasing linearly with Cr concentration. The study also identifies a critical Cr concentration beyond which the ferromagnetic phase becomes stable, with Curie temperatures exceeding room temperature from 14% Cr concentration, highlighting the material's suitability for practical applications. The ability to maintain ferromagnetic properties at ambient conditions underscores the potential of Cr-doped CaTe in developing efficient and reliable spintronic devices, such as magnetic sensors, memory devices, and components for quantum computing. These findings provide a foundation for future experimental and theoretical investigations aimed at optimizing Cr-doped CaTe for commercial spintronic applications.

REFERENCES

1. Terna, A.D.; Elemike, E.E.; Mbonu, J.I.; Osale, O.E.; Ezeani, R.O. The future of semiconductors nanoparticles: Synthesis, properties and applications. *Mater. Sci. Eng. B* **2021**, 272, 115363.
2. Dieny, B.; Prejbeanu, I.L.; Garello, K.; Gambardella, P.; Freitas, P.; Lehndorf, R.; Bortolotti, P. Opportunities and challenges for spintronics in the microelectronics industry. *Nat. Electron.* **2020**, 3, 446-459.
3. Marchenkov, V.V.; Irkhin, V.Y. Half-metallic ferromagnets, spin gapless semiconductors, and topological semimetals based on Heusler alloys: Theory and experiment. *Phys. Met. Metallogr.* **2021**, 122, 1133-1157.
4. Boutarfa, B.; Gous, M.H.; Meradji, H.; Boumaza, A.; Khenata, R. First principles study of the structural, elastic, electronic and optical properties of the ternary alloys $Ca_{0.75}Zn_{0.25}S$ and $Ca_{0.75}Zn_{0.25}Se$. *Comput. Condens. Matter* **2021**, 29, e00609.
5. Hakamata, S.; Ehara, M.; Kominami, H.; Nakanishi, Y.; Hatanaka, Y. Preparation of CaS: Cu, F thin-film electroluminescent devices with an emission including purple region. *Appl. Surf. Sci.* **2005**, 244, 469-472.
6. Luo, H.; Greene, R.G.; Ghandehari, K.; Li, T.; Ruoff, A.L. Structural phase transformations and the equations of state of calcium chalcogenides at high pressure. *Phys. Rev. B* **1994**, 50, 16232.

7. Roshan, S.R.; Kunduru, L.; Yedukondalu, N.; Sainath, M. Structure and lattice dynamics of calcium chalcogenides under high pressure. *Mater. Today: Proc.* **2018**, 5, 18874-18878.
8. Salam, M.M.A. Theoretical study of CaO, CaS and CaSe via first-principles calculations. *Results Phys.* **2018**, 10, 934-945.
9. Marinelli, F.; Lichanot, A. Elastic constants and electronic structure of alkaline-earth chalcogenides. Performances of various Hamiltonians. *Chem. Phys. Lett.* **2003**, 367, 430-438.
10. Straub, G.K.; Harrison, W.A. Self-consistent tight-binding theory of elasticity in ionic solids. *Phys. Rev. B* **1989**, 39, 10325.
11. Dadsetani, M.; Doosti, H. The linear optical properties for NaCl phase of calcium mono chalcogenides by density functional theory. *Comput. Mater. Sci.* **2009**, 45, 315-320.
12. Boucenna, S.; Medkour, Y.; Louail, L.; Boucenna, M.; Hachemi, A.; Roumili, A. High pressure induced structural, elastic and electronic properties of calcium chalcogenides CaX (X = S, Se and Te) via first-principles calculations. *Comput. Mater. Sci.* **2013**, 68, 325-334.
13. Boughrara, M.; M'Hid, A.A.; Kerouad, M. *Diluted Magnetic Semiconductors* in *Handbook of Semiconductors*, CRC Press: Boca Raton; **2024**; pp. 12-25.
14. Yuldashev, S.; Mukimov, K.; Eshonkulov, G.; Arslanov, A.; Xudoykulov, J. *Diluted Magnetic Semiconductors for Spintronics Applications* in *Proceedings of the International Conference on Low-Dimensional Advanced Materials (ICLODAM-24)*; Scientific Committee: Tashkent, Uzbekistan; **2024**.
15. Goumrhar, F.; Bahmad, L.; Benyoussef, A. Insight into structural, electronic, optoelectronic, dynamic, elastic, thermal and magnetic properties of pure and doped LiMgSb by nitrogen: Ab-initio calculations. *Mater. Sci. Semicond. Process.* **2024**, 181, 108596.
16. Goumrhar, F.; Mounkachi, O.; Bahmad, L.; Salmani, E.; Benyoussef, A. Magnetism in d^0 impurities doped CdTe: Ab-initio calculations. *Appl. Phys. A* **2020**, 126, 9.
17. Essajai, R.; Salmani, E.; Bghour, M.; Labrag, A.; Goumrhar, F.; Fahoume, M.; Ez-Zahraouy, H. Co-, Fe-, Ni-doped and co-doped rutile GeO_2: Insights from ab-initio calculations. *Commun. Theor. Phys.* **2022**, 74, 045701.
18. Akai, H. Fast Korringa-Kohn-Rostoker coherent potential approximation and its application to FCC Ni-Fe systems. *J. Phys. Condens. Matter* **1989**, 1, 8045.
19. Akai, H. Department of Physics, Graduate School of Science, Japan: Osaka University, Machikaneyama, Toyonaka 560-0043, **2002**. Available at: https://kkr.issp.u-tokyo.ac.jp/jp/.
20. Korringa, J. On the calculation of the energy of a Bloch wave in a metal. *Physica* **1947**, 13(6-7), 392-400.
21. Kohn, W.; Rostoker, N. Solution of the Schrödinger equation in periodic lattices with an application to metallic lithium. *Phys. Rev.* **1954**, 94, 1111.
22. Kohn, W.; Sham, L.J. Self-consistent equations including exchange and correlation effects. *Phys. Rev.* **1965**, 140, A1133.
23. Shiba, H. A reformulation of the coherent potential approximation and its applications. *Prog. Theor. Phys.* **1971**, 46, 77-94.
24. Perdew, J.P.; Burke, K.; Ernzerhof, M. Generalized gradient approximation made simple. *Phys. Rev. Lett.* **1996**, 77, 3865.
25. Dinh, V.A.; Sato, K.; Katayama-Yoshida, H. Dilute magnetic semiconductors based on wide bandgap SiO_2 with and without transition metal elements. *Solid State Commun.* **2005**, 136, 1-5.
26. Yoder, P. *Gallium nitride past, present, and future* in *1997 Proceedings IEEE/Cornell Conference on Advanced Concepts in High-Speed Semiconductor Devices and Circuits*, IEEE, **1997**; pp. 3-12.
27. Khaldi, A.; Bouarissa, N.; Tabourot, L. The pressure influence on structural parameters and elastic properties of rock-salt CaX (X = S, Se and Te) materials. *Chem. Phys. Impact* **2023**, 6, 100237.